Ultrasound in Med. & Biol., Vol. 40, No. 9, pp. 2207–2216, 2014

0301-5629/$ - see front matter

http://dx.doi.org/10.1016/j.ultrasmedbio.2014.05.005

● *Original Contribution*

COMPARING EFFICIENCY OF MICRO-RNA AND MRNA BIOMARKER LIBERATION WITH MICROBUBBLE-ENHANCED ULTRASOUND EXPOSURE

Alex Forbrich,* Robert Paproski,* Mary Hitt,† and Roger Zemp*

*Department of Electrical & Computer Engineering, University of Alberta, Edmonton, AB T6G 2V4, Canada; and †Department of Experimental Oncology, Cross Cancer Institute, University of Alberta, Edmonton, AB T6G 2V4, Canada

(*Received* 4 *December* 2012; *revised* 1 *May* 2014; *in final form* 7 *May* 2014)

Abstract—Blood biomarkers are potentially powerful diagnostic tools that are limited clinically by low concentrations, the inability to determine biomarker origin and unknown patient baseline. Recently, ultrasound has been shown to liberate proteins and large mRNA biomarkers, overcoming many of these limitations. We have since demonstrated that adding lipid-stabilized microbubbles elevates mRNA concentration an order of magnitude compared with ultrasound without microbubbles, *in vitro*. Unfortunately the large size of some mRNA molecules may limit efficiency of release and hinder efficacy as an ultrasound-liberated biomarker. We hypothesize that smaller molecules will be released more efficiently with ultrasound than larger molecules. Although investigation of large libraries of biomarkers should be performed to fully validate this hypothesis, we focus on a small subset of mRNA and micro-RNAs. Specifically, we focus on miR-21 (22 base pairs [bp]), which is upregulated in certain forms of cancer, compared with previously investigated mammaglobin mRNA (502 bp). We also report release of micro-RNA miR-155 (22 bp) and housekeeping rRNA S18 (1869 bp). More than 10 million additional miR-21 copies per 100,000 cells are released with ultrasound-microbubble exposure. The low- molecular-weight miR-21 proved to be liberated 50 times more efficiently than high-molecular-weight mammaglobin mRNA, releasing orders of magnitude more miR-21 than mammaglobin mRNA under comparable conditions. (E-mail: rzemp@ualberta.ca) **© 2014 World Federation for Ultrasound in Medicine & Biology.**

Key Words: **Biomarkers, Ultrasound, Microbubbles, micro-RNA, miRNA.**

INTRODUCTION

Biomarkers are important diagnostic and prognostic tools for clinicians to accurately and reliably evaluate many diseases, including cancer. Typically, tissue biopsies are necessary to properly assess the biomarkers in the tissue; however, biopsies are often technically challenging and risky because of the location of the tissue of interest. Blood-borne biomarkers have been researched extensively to limit or even to eliminate the need for tissue biopsies (Beachy and Repasky 2008; Chatterjee and Zetter 2005; Hanash et al. 2011; Tainsky 2009). Several protein blood biomarkers have been discovered with clinical utility, including carcinoembryonic antigen (CEA) in colon cancer, prostate-specific antigen (PSA) in prostate cancer and CA-125 in ovarian cancer (National Cancer Institute 2012; Tainsky 2009). These blood biomarkers have great potential for diagnostic and prognostic evaluation of diseases with little more than a blood sample; however, low biomarker concentration, inability to determine the source of detectable biomarkers and no patient baseline have all limited the introduction of blood-borne biomarkers into the clinic.

In 2009, D'Souza et al. (2009) demonstrated that 2-W/cm^2 ultrasound with 50% duty cycle could be applied to tissues *in vivo*, causing the release of CEA into the surrounding blood from a colorectal cancer cell line. Besides elevating biomarker levels in blood, this technique could also be used to determine the source of the biomarkers. A pre-ultrasound sample could be used as the patient baseline and any increase in the biomarker levels in a post-ultrasound sample could be attributed to the location of the applied ultrasound. This technique takes advantage of ultrasound–cell interactions that cause transient pores to form in the cell membrane, reversibly compromising its integrity and increasing its permeability, a process known as sonoporation. In 2010, Kaddur et al. (2010) used flow cytometry to demonstrate that microbubble-enhanced sonoporation could release enhanced green fluorescent protein from cells.

Address correspondence to: Roger Zemp, W2-101 ECERF, Edmonton, Alberta T6G 2V4. E-mail: rzemp@ualberta.ca

Before the papers by D'Souza et al. (2009) and Kaddur et al. (2010), the most common application of sonoporation has been to get molecules into cells for gene transfection and drug delivery (Chen et al. 2006; Delalande et al. 2012; Luo et al. 2008; Nomikou and McHale 2010). Because ultrasound can be directed and focused at specific tissues, sonoporation provides researchers with a method to noninvasively target specific tissues and transfect or release specific molecules *in vivo*. Sonoporation was found to induce pores sized at hundreds of nanometers (Zhou et al. 2009). Throughout the research into sonoporation it was found that microbubbles could substantially lower the required acoustic energy to induce sonoporation and increase the transfection efficiency. The exact mechanism for microbubbles enhancing sonoporation is not understood; however, there are several theories that explain this effect, including acoustic microstreaming caused by acoustic scattering around microbubbles (Marmottant and Hilgenfeldt 2003; Wu 2002), shock waves from collapsing microbubbles (Lokhandwalla and Sturtevant 2001) and microjet formation from asymmetric microbubbles collapsing near cells (Ohl et al. 2006; Prentice et al. 2005). Microbubble-enhanced sonoporation has been shown to create larger pores that can exceed a micrometer (Zhao et al. 2008). Recently, Fan et al. (2012) demonstrated transport kinetics of fluorescent molecules into a cell using microbubble-enhanced sonoporation. They demonstrated that a single bubble cavitating near cells could allow entry of impermeable propidium iodide and fluorescent calcein into the cells.

We have recently extended the concept of protein biomarker liberation using ultrasound to mRNA molecules and used lipid-stabilized microbubbles to further amplify the release of biomarkers by more than an order of magnitude compared with ultrasound alone (Forbrich et al. 2013). Microbubbles provide several advantages over ultrasound alone: (1) Microbubbles enhance sonoporation, reducing the cavitation energy necessary for the pores to form, which reduces the required acoustic intensity and duration needed for adequate biomarker liberation. (2) As contrast agents, ultrasound can detect single microbubbles (Klibanov et al. 2004) allowing for the development of a dual-mode high-contrast imaging biomarker liberation ultrasound system. (3) Microbubbles can be designed with ligands that target tissue-specific receptors, potentially causing an accumulation of bubbles near the tissue of interest. Coupled with a lower acoustic intensity and focused ultrasound, targeted microbubbles could limit biomarker liberation from unrelated tissues while substantially increasing the biomarker liberation from the tissue of interest.

The large size of many mRNA molecules may limit efficiency of release from cells. One goal of this paper is to investigate the hypothesis that smaller biomarker molecules will be released more efficiently compared with larger ones. A number of small molecule biomarker candidates could be considered; however, we choose to focus on micro-RNA (miRNA) as a related but smaller class of the mRNA biomarkers we previously investigated for ultrasound-aided liberation.

Recently there has been rising interest in miRNA as potential biomarkers for many diseases, including various forms of cancer (Fu et al. 2011; Jeffrey 2008; Kosaka et al. 2010; Lujambio and Lowe 2012; Ma et al. 2012; Sassen et al. 2008; Wittmann and Jäck 2010). miRNAs are small non-encoding RNAs, typically $<$25 nucleotides in length, which regulate the expression of many genes. In many cancers miRNAs are substantially dysregulated, creating a unique molecular profile capable of differentiating cancers and normal tissues (Lu et al. 2005; Lujambio and Lowe 2012). A unique 13-miRNA signature has been associated with chronic lymphocytic leukemia progression (Calin et al. 2005), and specific miRNA profiles have been correlated with estrogen and progesterone receptors, as well as human epidermal growth factor receptor 2—common receptors used to guide treatment and evaluate the prognosis of breast cancer patients (Fu et al. 2011; Iorio et al. 2005; Mattie et al. 2006).

This article presents a study of how miR-21, a 22-nucleotide RNA molecule, is liberated by ultrasound and microbubbles. The efficiency of the small-molecular-weight miR-21 biomarker is compared with our previously published work on mammaglobin mRNA. miR-21 is an ideal candidate miRNA biomarker because it is substantially upregulated in many cancers, including breast, colon, pancreatic, prostate and lung cancers (Volinia et al. 2006). We hypothesized that as the length of the nucleic acid decreases, the ability of ultrasound to amplify the release of the biomarker would increase. To exemplify this, we found that miR-21 is released more efficiently compared with our previous work on mammaglobin mRNA. Verification of this hypothesis, however, requires additional studies investigating a large library of nucleic biomarkers. Furthermore, we found that microbubbles can be used to obtain substantial increases in biomarker levels for miR-21. To our knowledge, the findings reported here are the first to quantitatively compare cellular release efficiency of different sized biomarker molecules and suggest that other small molecules that are candidate biomarkers for a range of diseases could offer enhanced diagnostic sensitivity when liberated by ultrasound-microbubble exposure.

METHODOLOGY

Microbubble preparation

Lipid-stabilized microbubbles were created by combining 350 μL lipid stock solution (27 mg/mL

1,2-dipalmitoyl-sn-glycero-3-phosphocholine [Sigma-Aldrich, St. Louis, MO, USA], 3 mg/mL 1,2-dipalmitoyl-sn-glycero-3-phosphoethanolamine [Sigma-Aldrich, St. Louis, MO, USA], and 100 mg/mL glucose dissolved in phosphate buffered saline (PBS)), 5 μL of 10% (w/v) albumin solution, and 50 μL of glycerol in a 1.5 mL tube, replacing the air in the tube with octafluoropropane gas (Electronic Fluorocarbons, LLC, Hopkinton, MA, USA), and shaking the tube for 30 seconds using a mechanical shaker (D-650 Amalgamator, TPC, City of Industry, CA, USA). This yielded an average concentration of 3.6×10^9 bubbles/mL with mean and mode diameters of 3.26 and 2.40 μm, respectively. This formulation was modified from Chen et al. (2006), who demonstrated the microbubbles formulation potential for *in vivo* experiments. Using this formulation allows future studies to investigate *in vivo* biomarker release using microbubbles without major modifications to the techniques presented here.

Sample preparation and collection

A procedure similar to that used by Forbrich et al. (2013) was used to allow direct comparison of mammaglobin mRNA with miR-21 miRNA. The procedure is pictorially summarized in Figure 1. In brief, each well of a 12-well plate was inoculated with 200,000 ZR-75-1 breast cancer cells (American Type Culture Collection) in 2 mL of RPMI with 10% fetal bovine serum and incubated for 3 days. Before insonifying a well, (1) the growth medium was aspirated, (2) the well was washed with PBS, (3) 1 mL of the growth medium with or without lipid-stabilized microbubbles (4×10^7 bubbles/mL) was added to the well, (4) the plate was gently mixed for 10–15 sec, and (5) a 480 μL pre-ultrasound sample was taken. The 12-well plate was then half-immersed in a 37°C water bath directly above a 1 MHz, unfocused ultrasound transducer (SP100 Sonoporator, Sonidel Limited, Raheny Dublin, Ireland). Acoustic parameters ranged from 0.1 to 5 W/cm^2 (spatial-average, temporal peak [SATP] intensity), 25%–50% duty cycle, and 1- to 30-min exposure duration. The transducer was constantly moved during sonicating to interrogate all the cells. After sonication and 10–15 sec of mixing, a 480 μL post-ultrasound sample was taken. The samples were centrifuged at 16,000 $\times$ *g* and 450 μL of the supernatant was transferred to a new vial, which was flash frozen in liquid nitrogen and stored in a −80°C freezer until later processing. Each experimental setting was conducted at least three times.

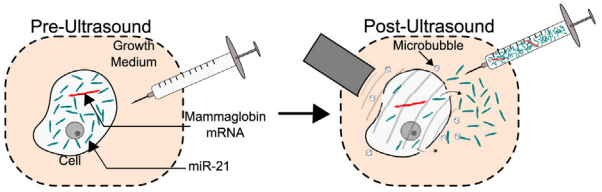

Fig. 1. Biomarker liberation procedure. Pre- and post-ultrasound medium samples are taken and compared.

The acoustic intensity calibration for the SP100 ultrasound system was verified by submerging a hydrophone (HNP-400, Onda, Sunnyvale, CA, USA) and the SP100 system in a water tank and recording the detected pressures. References to the acoustic intensity throughout this paper refer to the system settings. The acoustic intensity at the cell layer within the well was also determined by placing the tip of the hydrophone into ~500 μL PBS in the 12-well plate and exposing the well to ultrasound. The hydrophone was moved in a raster pattern to obtain two-dimensional (2-D) pressure profiles within the well under various conditions.

Cell viability

After the biomarker liberation experiment, PBS and trypsin were used to collect all cells from each well. The centrifuged post-ultrasound vial was washed with PBS to collect any cells that detached during the experiment. Cell viability was assessed with trypan blue staining and a hemocytometer after an hour to allow the resealing of pores formed during sonication because many groups have reported that small-pore resealing occurs within a few minutes (Deng et al. 2004; Yang et al. 2008). Larger pores may not have resealed in this time (Zhao et al. 2008) and may allow trypan blue to stain the cells; these cells are considered dead in our analysis.

miR-21 biomarker liberation as a result of cell death

Cell incubation with hydrogen peroxide (H_2O_2) was performed to induce cell death and quantify the number of miR-21 copies released as a result of cell death. The ZR-75-1 cells (cultured and plated in 12-well plates as described earlier) were incubated with hydrogen peroxide for 30 min (the maximum length of the ultrasound experiments) at H_2O_2 concentrations varying from 10 μM to 500 mM. Samples of the medium were collected and analyzed for cell death and biomarker liberation as previously described.

Ideally it would be preferred to have some chemical treatment that would kill cells but not lyse them and not affect RNA levels as a control treatment to compare with ultrasound treatments. Unfortunately many chemical treatments may affect RNA expression levels. Our approach was to use H_2O_2 (which is shown to induce apoptosis) as a chemical treatment and correct for the alteration in RNA expression levels using a correction factor. To account for the effects of H_2O_2 either on miR-21 expression in cells or on miR-21 itself, ZR-75-1 cells incubated with or without H_2O_2 were lysed (using

Qiazol as part of the RNA purification kit protocol) and RNA levels were compared. Using this data, a correction factor (miR-21 from Qiazol-lysed cells incubated with H_2O_2 divided by miR-21 from lysed cells incubated without H_2O_2) is obtained and applied to the H_2O_2 release data in all figures. This correction factor is meant to account for reduction in RNA levels associated with H_2O_2, while still having some means to compare RNA release from ultrasound treatment.

It could be argued that H_2O_2 treatment is a biased control because it does not bring about mechanical stresses and could instead induce changes in mRNA expression. For this reason we accounted for mRNA expression level changes caused by H_2O_2 and also included mechanical lysing as an alternate control. For mechanical lysis, we used a Pro300 A Homogenizer (Pro Scientific, 8 bursts of ~20s at 18,000 RPM) to mechanically lyse cells. Trypan blue staining confirmed that >95% of cells were dead.

Biomarker quantification

Absolute quantification of the miR-21 miRNA was completed using a standard TaqMan procedure. First, total RNA was purified into a 30-μL eluate using a total RNA purification kit (miRNeasy Mini Kit, Qiagen, Mississauga, ON, Canada). Second, miR-21 was reverse transcribed by using TaqMan MicroRNA Reverse Transcription Kit (Applied Biosystems, Burlington, ON, Canada). Third, TaqMan probes and primers specific for miR-21 were combined with the miR-21 complimentary deoxyribonucleic acid (DNA), TaqMan Universal Master Mix II (Applied Biosystems, Burlington, ON, Canada) and analyzed using the 7900HT Fast Real-Time PCR System (Applied Biosystems, Burlington, ON, Canada). Standard curves were created for miR-21 by creating a known concentration of RNA primers (GenScript, Piscataway, NJ, USA) with the miR-21 nucleotide sequence. This standard curve is used in analysis to determine the number of miR-21 copies present in the reverse transcribed solution. To account for the dilutions in the analysis, a correction factor of 7.45 is used to determine the number of copies in the original 500 μL pre- and post-ultrasound samples. One-way and two-way analysis of variance (ANOVA) and Tukey honest significant difference (HSD) test were used to determine statistical significance.

RESULTS AND DISCUSSION

Although miR-21 was found naturally in the growth medium, the subtraction of the pre-ultrasound sample from the post-ultrasound sample accounts for ultrasound-aided release relative to the baseline. Control experiments were conducted to account for the natural release of miR-21 over the length of the experiment. After 30 min (the maximum length of the experiments) there were $6 \times 10^6 \pm 2 \times 10^6$ miR-21 copies released per 100,000 cells. The natural release of miR-21 was 1–2 orders of magnitudes less than the amount released by ultrasound and microbubbles.

Figure 2 shows a 2-D raster scan of the pressure profile within a 12-well plate while the SP100 ultrasound system delivered 2 W/cm^2 (SATP averaged over the transducer aperture) at 50% duty cycle. The measured spatial peak, temporal peak (SPTP) intensity was 12.1 W/cm^2 with a full-width half-maximum (FWHM) of ~3.5 mm. Averaging over the entire effective radiating area, we found the SATP intensities in the well were ~2.95 W, nearly a 50% increase in intensity compared with the reported value. These results are consistent with results from Kinoshita and Hynynen (2007) and Hensel et al. (2011), who found intensities can range by a factor of four as a result of the formation of standing waves in the well. Variations in the volume of liquid in the well, slight streaming effects and transducer motion constantly changed the location of standing wave nodes and cause a large variation of the measured intensities. The hydrophone measured a symmetric acoustic pressure wave allowing for the determination of the peak negative pressure (PNP) and mechanical index (MI) – crucial values for cavitation. PNP is determined by $(2\rho_0 c_0 I)^{1/2}$, where ρ_0 and c_0 is the density and speed of sound in the liquid, respectively, and I is the intensity. MI is calculated as PNP/$f^{1/2}$ where f is the frequency of the ultrasound in MHz. Reported intensities of 0.1, 0.3, 0.5, 1, 3 and 5 W/cm^2 thus correspond to PNPs of 0.05, 0.09, 0.12, 0.17, 0.30, 0.39 MPa_{PNP} and MIs of 0.05, 0.09, 0.12, 0.17, 0.30, 0.39, respectively. All intensities on the figures refer to the SP100 system settings;

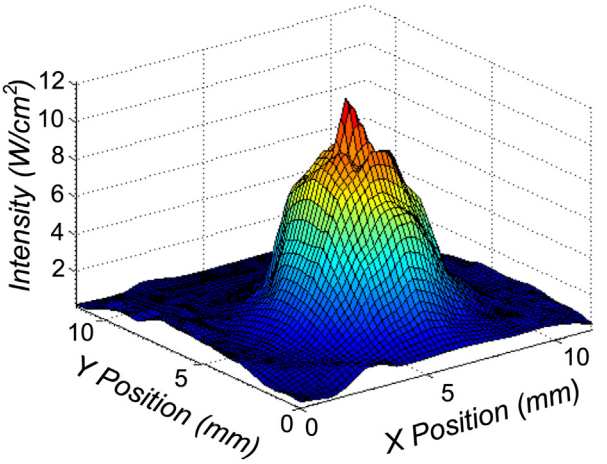

Fig. 2. A pressure profile of a 1-MHz unfocused transducer within a well of a 12-well plate. The SP100 system lists the intensity at 2 W/cm^2.

however, hydrophone measurements reveals that the intensity within the well could range from one- to fourfold greater, consistent with Kinoshita and Hynynen (2007) and Hensel et al. (2011).

Microbubble cavitation was confirmed through microscopy and hydrophone measurements. Using a 20-cycle burst of 1 MHz ultrasound, we found that the intensity required to destroy more than 95% of the bubbles was more than 14.8 W/cm^2. However, with enough cycles even the lowest intensity ultrasound used in this paper (0.1 W/cm^2) was able to destroy the microbubbles.

The results of the H_2O_2 studies are presented in Figure 3. Figure 3a shows the cytotoxicity and was used to find appropriate H_2O_2 concentrations to determine the cell death equivalent biomarker released used in Figures 4, 5, and 6. Figure 3b shows the biomarker liberation as a result of incubation with the H_2O_2. Although the mechanisms of biomarker liberation caused by ultrasound-microbubble exposure and H_2O_2 incubation are not necessarily identical, these experiments give a good idea as to the contribution cell death has on the amount of biomarkers liberated. As a constant source of chemical, oxidative stress, high levels of H_2O_2 have previously been shown to dysregulate the expression of genes (Chuang et al. 2002) and can potentially damage DNA (Linley et al. 2012). This is believed to be a dominant mechanism of cell necrosis. We used H_2O_2 treatment as a chemical means of inducing cell death in contrast to the mechanical mechanisms believed to operate in ultrasound-microbubble interactions. H_2O_2 chemical stresses can also affect miRNA expression, and indeed we found that H_2O_2 treatment reduced miR-21 levels. This effect is accounted for by comparing gene expression of lysed cells incubated with and without H_2O_2. Comparing miR-21 expression in Qiazol-lysed cells incubated with or without H_2O_2 indicated that the cells incubated with H_2O_2 expressed $\sim$1.8 $\pm$ 0.2-fold less than cells incubated without H_2O_2. A correction factor was applied to the H_2O_2 data shown in the figures to account for this expression difference. It should be noted that the mechanism of H_2O_2 on biomarker release is unclear and could be a topic of further research.

In addition to the use of H_2O_2 to chemically lyse cells as a control treatment, we also considered mechanical lysing treatments as an alternate control. The miR-21 biomarker concentration from mechanically lysed cells (via homogenizer) was 2.6 $\pm$ 0.3-fold less than the cells lysed with the purification kit and 1.4-fold less than H_2O_2 treatments. In a sense these mechanical lysing data were counterintuitive to us because we expected mechanical lysing to release cell contents and present total RNA levels. It is likely that exosomes, microvesicles and cell fragments created or released during the homogenization procedure and containing RNA were removed during the centrifugation step common to all post-treatment protocols. As a reference for comparison for Figures 4, 5 and 6, a maximum of 4.2 $\times$ 10^8 copies per 100,000 cells could be liberated as determine by complete mechanical lysis of the cells using a homogenizer and is indicated on Figures 4–6 by a solid black line.

The effect of duty cycle on miR-21 liberation with and without microbubbles was examined by applying 1 MHz, 2 W/cm^2 ultrasound for 1 min (Fig. 4). Without microbubbles, cell viability was measured at 92.1 $\pm$ 2.0 and 89.5 $\pm$ 1.0%, whereas with microbubbles cell viability was measured at 70.2 $\pm$ 6.5 and 69.9 $\pm$ 2.2% at 25% and 50% duty cycle, respectively. The cell death equivalent biomarker liberation shown in Figure 3 shows that only a small portion of biomarker liberation is due to cell death. Two-way ANOVA shows that both microbubbles ($p < 0.001$) and duty cycle ($p < 0.05$) have a statistically significant effect on biomarker liberation with no significant interaction between the two variables. As in previous work (D'Souza et al. 2009; Forbrich et al. 2013), high-duty cycle is a crucial factor when working with ultrasound alone ($p < 0.05$); however, the addition of microbubbles allows even low-duty cycle ultrasound to exceed the miR-21 liberation at high-duty cycle ultrasound without microbubbles. Ultrasound with

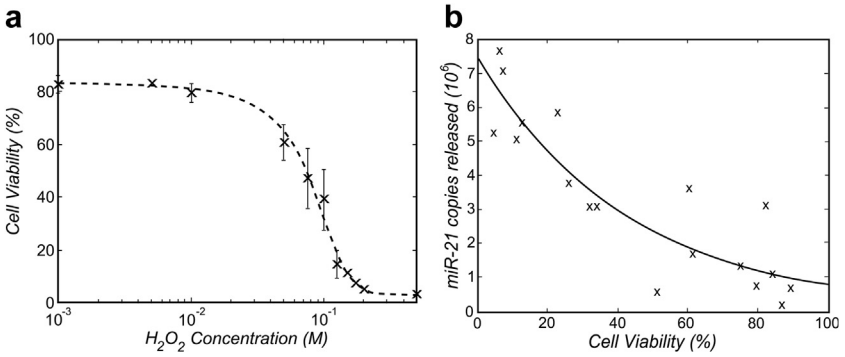

Fig. 3. (a) Hydrogen peroxide–induced cell death and (b) miR-21 liberation as a result of hydrogen peroxide incubation.

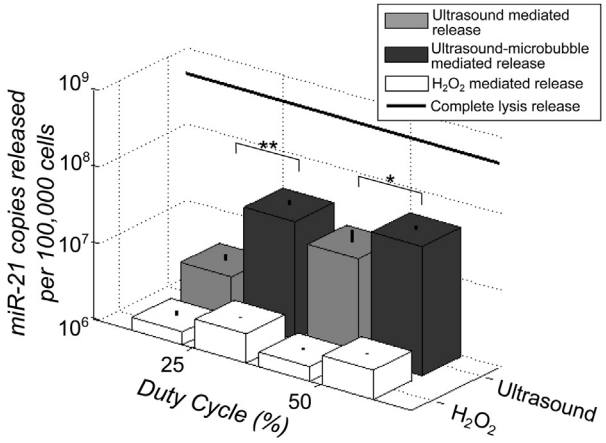

Fig. 4. Ultrasound duty cycle and microbubbles on miR-21 liberation. Biomarker release from ZR-75-1 cells exposed to either a 1-MHz, 2-W/cm^2 unfocused ultrasound transducer for 1 min with or without microbubbles (*dark gray* and *light gray bars*, respectively) or exposed to H_2O_2 without ultrasound. *White bars* represent miR-21 release as a result of H_2O_2 exposure at similar cell viabilities as corresponding ultrasound experiments (cell death equivalent biomarker release). The *solid black line* represents the maximum possible miR-21 release. *Asterisks (*)* represent statistical significance as determined by two-way ANOVA and Tukey HSD analysis. Both microbubbles ($p < 0.001$) and duty cycle ($p < 0.05$) have statistical significance without statistical interaction ($p \approx 0.92$). Note: H_2O_2 treated cells were not exposed to ultrasound.

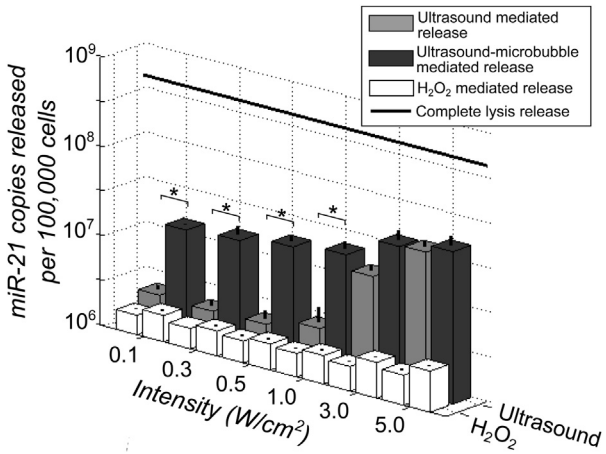

Fig. 5. Ultrasound intensity and microbubbles on miR-21 liberation. Biomarker release from ZR-75-1 cells exposed to either a 1-MHz, 50% duty cycle unfocused ultrasound transducer for 10 min with or without microbubbles (*dark gray* and *light gray bars*, respectively) or exposed to H_2O_2 without ultrasound. *White bars* represent release caused by H_2O_2 exposure at similar cell viabilities as corresponding ultrasound experiments (cell death equivalent biomarker release). The *solid black line* represents the maximum possible miR-21 release. *Asterisks (*)* represent statistical significance as determined by two-way ANOVA and Tukey HSD analysis. Both microbubbles and intensity have statistical significance ($p < 0.01$) without statistical interaction ($p \approx 0.44$). Note: H_2O_2 treated cells were not exposed to ultrasound.

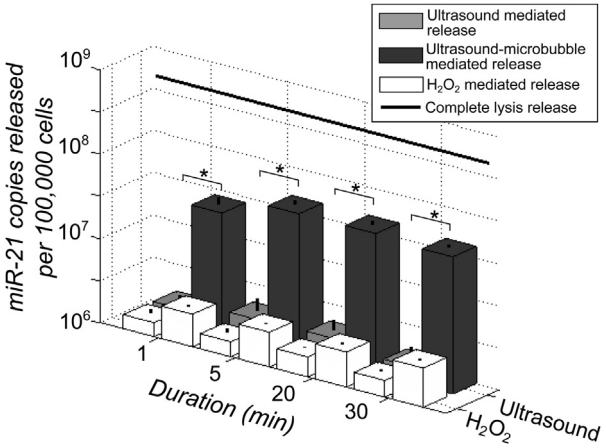

Fig. 6. Ultrasound duration and microbubbles on miR-21 liberation. Biomarker release from ZR-75-1 cells exposed to either a 1-MHz, 2-W/cm^2 (50% duty cycle) unfocused ultrasound transducer with or without microbubbles (*dark gray* and *light gray bars*, respectively) or exposed to H_2O_2 without ultrasound. *White bars* represent release caused by H_2O_2 exposure at similar cell viabilities as corresponding ultrasound experiments (cell death equivalent biomarker release). The *solid, thick line* represents the maximum possible miR-21 release. *Asterisks (*)* represent statistical significance as determined by two-way ANOVA and Tukey HSD analysis. The addition of microbubbles caused statistically significant increases in miR-21 release ($p < 0.01$), and duration had less statistical significance ($p \approx 0.05$), with minimal interaction between these parameters ($p \approx 0.069$). Comparing no microbubbles with microbubbles reveals statistical significance ($p < 0.05$). Note: H_2O_2 treated cells were not exposed to ultrasound.

microbubbles increase miR-21 liberation by 6.4- and 2.6-fold at 25% and 50% duty cycles, respectively, compared with ultrasound alone ($p < 0.05$). The effect of increasing duty cycle from 25% to 50% is reduced when microbubbles are present only providing a 1.4-fold increase in copies, whereas a five-fold increase is seen with ultrasound alone. Previous publications (D'Souza et al. 2009; Forbrich et al. 2013) indicated that protein and mRNA biomarkers require high-duty cycle to sufficiently release biomarkers—CEA liberation wasn't achieved even at acoustic intensities of 6 W/cm^2 at 20% duty cycle (D'Souza et al. 2009). However, these data show that it may be possible to examine an array of important miRNA at clinically used lower duty cycles and intensities.

Using microbubbles may be an important factor to reduce the required duty cycle and may lead to current clinical ultrasound systems being capable of releasing biomarkers into the blood. Furthermore, tissue damage is a concern that would be mitigated by reducing the duty cycle and intensity. Because microbubbles reduce both the duty cycle (Fig. 4) and the intensity (Fig. 5) required, ultrasound-aided biomarker release may show promise at clinical diagnostic limits for ultrasound

exposure. Alternatively, novel ultrasound systems could be designed to handle high-duty cycle biomarker liberation. As suggested in the introduction, microbubbles give high contrast—in fact, single microbubble sensitivity (Klibanov et al. 2004)—in ultrasound imaging; hence, an ultrasound system could be dual-purposed for low-duty cycle imaging and high-duty cycle biomarker release.

Although no substantial increase is seen at 50% duty cycle compared with 25% duty cycle when microbubbles are present, all future experiments are conducted at 50% duty cycle to be consistent with other protocols. Slightly lower, but still significant ($p < 0.05$), numbers of miR-21 miRNA copies are expected at 25% duty cycle with microbubbles and may be used if heating and power delivered to the tissue becomes an issue. Higher duty cycles and continuous ultrasound were not examined because transducer and tissue overheating and power delivery were concerns.

Figure 5 shows how miR-21 release is substantially increased with microbubbles and moderate intensity. Cells were sonicated for 10 min at 50% duty cycle at varying acoustic intensities. Without microbubbles, cell viability was measured at 86.8 ± 3.3, 85.8 ± 1.6, 84.1 ± 1.5, 82.3 ± 3, 81.0 ± 0.7 and 74.8 ± 2.64% at 0.1, 0.3, 0.5, 1.0, 3.0 and 5.0 W/cm^2, respectively. With microbubbles, cell viability was measured at 79.0 ± 3.6, 80.8 ± 1.0, 79.5 ± 2.4, 76.6 ± 0.5, 68.4 ± 0.7 and 62.3 ± 3.2% at 0.1, 0.3, 0.5, 1.0, 3.0 and 5.0 W/cm^2 ultrasound intensity, respectively. Results from the H_2O_2 studies show that the contribution of biomarker liberation from cell death is minimal compared with the total amount of miR-21 released because of ultrasound-microbubble exposure. Two-way ANOVA shows that both microbubbles ($p < 0.01$) and acoustic intensity ($p < 0.01$) have statistically significant effects on biomarker liberation. At low acoustic intensities (<1 W/cm^2) the microbubbles produce dramatic increases in miR-21 release ($p < 0.05$), causing nearly an order of magnitude increase in the miR-21 concentration compared with no microbubbles. However, at high acoustic intensity (5 W/cm^2) both ultrasound alone and with microbubbles release a high concentration of miR-21 into the surrounding medium, causing only 1.2-fold increase in miR-21 concentrations compared with ultrasound alone. The most substantial increase in copy count as a result of microbubbles is seen at 3 W/cm^2, where more than 25 million miR-21 molecules are released per 100,000 cells. The results follow the same trend as the mammaglobin mRNA (Forbrich et al. 2013); however, the copies released are three orders of magnitude greater for miR-21.

Figure 5 shows that acoustic intensity is an important factor for biomarker liberation ($p < 0.05$). With and without microbubbles, the biomarker release substantially increases after 1 W/cm^2, and by 5 W/cm^2 the biomarker liberation without microbubbles is nearly identical to the with-microbubble scenario. The substantial increase after 1 W/cm^2 may be due to the acoustic intensity being great enough to induce cavitation without immediate microbubble destruction, whereas the minute differences at 5 W/cm^2 most likely are due to inertial cavitation of the microbubbles early in the ultrasound therapy limiting microbubble–cell interaction duration. Although the large biomarker liberation at 5 W/cm^2 is ideal, our results indicate that cell death starts to increase drastically after 1 W/cm^2. At low acoustic intensities (≤1 W/cm^2) there is a substantial difference between non-microbubble and microbubble experiments ($p < 0.05$). This most likely is due to microbubbles undergoing stable cavitation instead of inertial cavitation and therefore remaining in the growth media throughout the entire experiment. Furthermore, the continual presence of microbubbles throughout the experiment at low intensities may cause microstreaming effects that place sheer stress in the cell membrane, causing small pores to form (Marmottant and Hilgenfeldt 2003; Wu 2002). Larger pores can form at high intensity because of microbubble collapse creating microjets and shock waves (Lokhandwalla and Sturtevant 2001; Ohl et al. 2006; Prentice et al. 2005; Zhao et al. 2008). The larger pores created at high intensity may allow the biomarkers to more easily diffuse out of the cell, thus giving rise to higher biomarker liberation.

Figure 6 shows that miR-21 concentrations peak at 5 min; however, unlike mammaglobin mRNA, which decreased by more than 45% over 30 min, miR-21 remains relatively constant for 30 min in the growth medium, only decreasing by 7% (not statistically significant, $p > 0.05$). This difference may be due to miRNA being more stable than mRNA outside of cells. Without microbubbles, the miR-21 concentration slowly rises and plateaus within 5 min. However, with microbubbles there is a statistically significant ($p < 0.01$) increase in miR-21 concentration (18- to 25-fold increase compared with no microbubbles). Although the reason for the decrease in concentration is unknown, the early peak in miR-21 concentration is desirable for *in vivo* experiments. Furthermore, Figure 6 demonstrates the high stability of miR-21, which make miRNA more desirable than mammaglobin mRNA for lengthy procedures. Without microbubbles, cell viability was 89.5 ± 1.0, 90.9 ± 3.4, 84.9 ± 5.5 and 82.2 ± 0.8% at 1, 5, 20 and 30 min exposure duration, respectively. With microbubbles, cell viability was 69.9 ± 2.2, 67.3 ± 7.9, 66.8 ± 4.1 and 61.8 ± 3.4% at 1, 5, 20 and 30 min exposure duration, respectively.

Examining miRNAs presents several advantages over other potential biomarkers, including proteins and mRNAs. Because many miRNAs regulate the expression of more than one gene, an unusual level of miRNA may be indicative of more than one abnormally expressed gene. Simultaneous profiling of a number of biomarkers could offer improved sensitivity and specificity. As with our previous mRNA study (Forbrich et al. 2013), our present study using miRNA uses TaqMan to quantify the levels of RNA, which has high specificity, has more than seven orders of magnitude dynamic range, and most importantly for blood biomarkers, has near single-copy sensitivity. Overall our *in vitro* results indicated that miRNAs have great potential as biomarkers. Their small size and low molecular weight allow miRNAs to more easily diffuse out of cells compared with mRNA. The number of copies released of miR-21 is orders of magnitude greater than that of mammaglobin mRNA (Fig. 7a). Quantifying the number of RNA molecules present in a solution of lysed ZR-75-1 cells resulted in ~82 mammaglobin mRNA copies per cell and ~1110 miR-21 copies per cell. This implied that only 0.4% and 20.3% of the mammaglobin mRNA and the miR-21 molecules in the cells were released into the growth media, respectively (using data for a 1 MHz unfocused transducer at 1 W/cm^2, 50% duty cycle and 10-min exposure), when microbubbles were present as depicted in Figure 7b. This supports our hypothesis that biomarker liberation is related to the size of the molecule in that smaller molecules (miR-21, 22 bases) inside cells are more easily liberated than larger molecules (mammaglobin mRNA, 502 bases).

Although the concentration of microbubbles used in our *in vitro* studies is not attainable *in vivo*, a continuous intravenous injection of microbubbles would allow the microbubbles to continuously flow throughout the target tissue, replenishing the microbubbles that burst. This could allow for enhanced biomarker liberation. Targeted microbubbles could also be designed with ligands to bind to the target tissue, causing a buildup of microbubbles and a potentially large biomarker release. Furthermore, primary radiation forces from the ultrasound can act on the microbubbles *in vivo*, causing microbubble translation, moving the microbubbles closer to the blood vessel walls and the target tissue—potentially increasing the biomarker release and binding efficiency of targeted microbubbles. Given that the total number of cells per well is approximately 800,000 at the time of the experiments, the ratio of bubbles to cells is quite high at 50 to 1. This observation should be tempered with the fact that cells are growing in a monolayer, whereas microbubbles are distributed throughout the volume of the growth medium. Microscopy of the cell monolayers show that there are significantly fewer microbubbles visible compared with cells; however, because of acoustic streaming and mixing effects it is difficult to know the number of microbubbles that interact with each cell.

Microbubbles are advantageous in many aspects; however, several limitations will exist when translating this work into animal models. Microbubbles are intravascular agents and are too big to escape the vasculature. Endothelial cell lining increases the microbubble-tumor cell separation and may reduce the effects of ultrasound-microbubble interaction on cancerous tissues. Sub-micron microbubbles (Kim et al. 2010; Yin et al. 2012) and phase-change nanodroplets (Sheeran et al. 2011; Wilson et al. 2012) have been developed that can extravasate out the leaky vasculature surrounding tumors, providing passive accumulation. Studies should be designed to

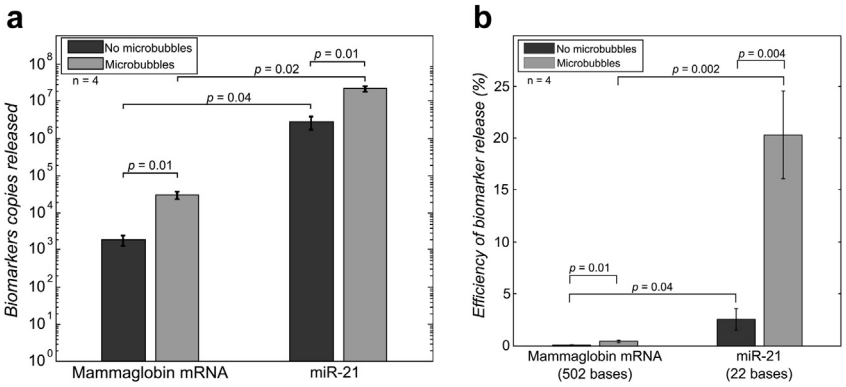

Fig. 7. Comparison of mammaglobin mRNA and miR-21 liberation using a 1-MHz unfocused transducer to expose ZR-75-1 breast cancer cells to 10 min of 1-W/cm^2, 50% duty cycle ultrasound. (a) Copies released on a logarithmic scale. (b) Biomarker liberation efficiency. The number of biomarkers per cell was determined and used to estimate the efficiency of biomarker release. Two-way ANOVA indicates that both the addition of microbubbles and the type of biomarker are statistically significant ($p < 0.05$) and that there is significant interaction ($p < 0.05$).

examine how well these microbubbles work for biomarker liberation. Analyzing miR-21 levels alone does not provide great insight for diagnostic classification and prognostic evaluation; hence, an array of miRNAs must be examined to determine the diagnostic ability of this technique. Future studies should investigate larger arrays of RNA and protein to examine the diagnostic potential of this technique. Preliminary results using the housekeeping rRNA 18S (1869 bp) and the micro-RNA miR-155 (22 bp) verify that this process is not unique to miR-21. Using 1 MHz, 1 W/cm^2, 50% duty cycle ultrasound for 10 min, a fold increase of up to 1.24 ± 0.16 and 2.56 ± 0.48 was measured without microbubbles, whereas with microbubbles a fold increase of up to 2.36 ± 0.09 and 6.06 ± 0.12 was measured for 18S and miR-155, respectively. miR-155 was found to be expressed at very low concentrations in the ZR-75-1 cells compared with miR-21; hence, only a small fold increase is seen. Ultrasound-induced release efficiency may depend not only on molecular size but also on concentration gradients across cell membranes, intracellular packaging of molecules and other complex effects. Future investigation should assess how concentration gradients and other factors effect biomarker liberation.

There has been much research into how biomarkers are shed into the bloodstream; however, the exact mechanism is not well understood. Extracellular RNAs have been shown to be released as free-circulating molecules, exosomes, microvesicles, apoptotic bodies and ribonucleoproteins (Arroyo et al. 2011; Zandberga et al. 2013). Because many studies have reported that ultrasound-microbubble interaction near cells induces sonoporation, we speculate that the primary mechanism of biomarker liberation from cells as a result of ultrasound and ultrasound-microbubble exposure is sonoporation. However, more investigation is needed to determine the exact mechanisms for biomarker release, and this is left for future studies.

Overall, miRNAs have great potential as diagnostic markers and this technique may help release biomarkers into the blood allowing for minimally invasive diagnostics. This ultrasound-enhanced liberation technique applied to miRNAs may aid diagnostic and prognostic medicine because (1) miRNAs are small, low-molecular-weight molecules that can diffuse out of cells with more than 50-fold higher efficiency than previously investigated mammaglobin mRNA using ultrasound-microbubble exposure; (2) as a model miRNA, miR-21 has been detected with several orders of magnitude increase in copy number compared with background levels, making detection and reproducibility promising; and (3) miRNAs are much more stable than mammaglobin mRNA based on our previous work.

CONCLUSIONS

Our findings indicate that miR-21 is released much more efficiently than mammaglobin mRNA and support the hypothesis that ultrasound-mediated biomarker liberation of smaller molecules is more efficient than larger molecules. Although more investigation is needed to verify this hypothesis for a large library of biomolecules, these data suggest that other smaller molecules that are candidate biomarkers for a range of diseases may offer enhanced diagnostic sensitivity when liberated by ultrasound-microbubble exposure compared with larger molecules, an effect that may be further amplified by microbubbles.

Acknowledgments—We gratefully acknowledge funding from the Alberta Cancer Research Institute (ACB 23728 and AHS CRCFA 24777); Natural Sciences and Engineering Research Council of Canada (355544-2008, 375340-2009, STPGP 396444); Terry Fox Foundation and the Canadian Cancer Society (TFF 019237, TFF 019240, CCS 2011-700718); the Canada Foundation for Innovation, Leaders Opportunity Fund (18472); Alberta Advanced Education & Technology, Small Equipment Grants Program (URSI09007SEG); and University of Alberta Startup Funds. We acknowledge Carol Cass, Ronald Moore, and John Lewis for providing wet lab facilities. We also acknowledge John Mackey and Jean Deschenes for helpful discussions regarding breast cancer biomarkers.

REFERENCES

Arroyo JD, Chevillet JR, Kroh EM, Ruf IK, Pritchard CC, Gibson DF, Mitchell PS, Bennett CF, Pogosova-Agadjanyan EL, Stirewalt DL, Tait JF, Tewari M. Argonaute2 complexes carry a population of circulating microRNAs independent of vesicles in human plasma. Proc Natl Acad Sci USA 2011;108(12):5003–5008.

Beachy SH, Repasky EA. Using extracellular biomarkers for monitoring efficacy of therapeutics in cancer patients: An update. Cancer Immunol Immunother 2008;57(6):759–775.

Calin GA, Ferracin M, Cimmino A, Di Leva G, Shimizu M, Wojcik SE, Iorio MV, Visone R, Sever NI, Fabbri M, Iuliano R, Palumbo T, Pichiorri F, Roldo C, Garzon R, Sevignani C, Rassenti L, Alder H, Volinia S, Liu CG, Kipps TJ, Negrini M, Croce CM. A MicroRNA signature associated with prognosis and progression in chronic lymphocytic leukemia. N Engl J Med 2005;353(17):1793–1801.

Chatterjee SK, Zetter BR. Cancer biomarkers: Knowing the present and predicting the future. Future Oncol 2005;1(1):37–50.

Chen S, Ding JH, Bekeredjian R, Yang BZ, Shohet RV, Johnston SA, Hohmeier HE, Newgard CB, Grayburn PA. Efficient gene delivery to pancreatic islets with ultrasonic microbubbles destruction technology. Proc Natl Acad Sci USA 2006;103(22):8469–8474.

Chuang YY, Chen Y, Gadisetti, Chandramouli VR, Cook JA, Coffin D, Tsai MH, DeGraff W, Yan H, Zhao S, Russo A, Liu ET, Mitchell JB. Gene expression after treatment with hydrogen peroxide, menadione, or t-butyl hydroperoxide in breast cancer cells. Cancer Res 2002;62(21):6246–6254.

D'Souza AL, Tseng JR, Pauly KB, Guccione S, Rosenberg J, Gambhir SS, Glazer GM. A strategy for blood biomarker amplification and localization using ultrasound. Proc Natl Acad Sci USA 2009;106(40):17152–17157.

Delalande A, Postema M, Mignet N, Midoux P, Pichon C. Ultrasound and microbubble-assisted gene delivery: recent advances and ongoing challenges. Ther Deliv 2012;3(10):1199–1215.

Deng CX, Sieling F, Pan H, Cui J. Ultrasound-induced cell membrane porosity. Ultrasound Med Biol 2004;30(4):519–526.

Fan Z, Liu H, Mayer M, Deng CX. Spatiotemporally controlled single cell sonoporation. Proc Natl Acad Sci USA 2012;109(41):16486–16491.

Forbrich A, Paproski R, Hitt M, Zemp R. Microbubble-enhanced ultrasound amplification of mRNA biomarkers in vitro. Ultrasound Med Biol 2013;39(6):1087–1093.
Fu SW, Chen L, Man YG. miRNA Biomarkers in breast cancer detection and management. J Cancer 2011;2:116–122.
Hanash SM, Baik CS, Kallioniemi O. Emerging molecular biomarkers–blood-based strategies to detect and monitor cancer. Nat Rev Clin Oncol 2011;8(3):142–150.
Hensel K, Mienkina MP, Schmitz G. Analysis of ultrasound fields in cell culture wells for in vitro ultrasound therapy experiments. Ultrasound Med Biol 2011;37(12):2105–2115.
Iorio MV, Ferracin M, Liu CG, Veronese A, Spizzo R, Sabbioni S, Magri E, Pedriali M, Fabbri M, Campiglio M, Ménard S, Palazzo JP, Rosenberg A, Musiani P, Volinia S, Nenci I, Calin GA, Querzoli P, Negrini M, Croce CM. MicroRNA gene expression deregulation in human breast cancer. Cancer Res 2005;65(16):7065–7070.
Jeffrey SS. Cancer biomarker profiling with microRNAs. Nat Biotechnol 2008;26(4):400–401.
Kaddur K, Lebegue L, Tranquart F, Midoux P, Pichon C, Bouakaz A. Transient transmembrane release of green fluorescent proteins with sonoporation. IEEE Trans Ultrason Ferroelectr Freq Control 2010;57(7):1558–1567.
Kim C, Qin R, Xu JS, Wang LV, Xu R. Multifunctional microbubbles and nanobubbles for photoacoustic and ultrasound imaging. J Biomed Opt 2010;15(1):010510.
Kinoshita M, Hynynen K. Key factors that affect sonoporation efficiency in in vitro settings: the importance of standing wave in sonoporation. Biochem Biophys Res Commun 2007;359(4):860–865.
Klibanov AL, Rasche PT, Hughes MS, Wojdyla JK, Galen KP, Wible JH Jr, Brandenburger GH. Detection of individual microbubbles of ultrasound contrast agents: Imaging free-floating and targeted bubbles. Invest Radiol 2004;39(3):187–195.
Kosaka N, Iguchi H, Ochiya T. Circulating microRNA in body fluid: A new potential biomarker for cancer diagnosis and prognosis. Cancer Sci 2010;101(10):2087–2092.
Linley E, Denyer SP, McDonnell G, Simons C, Maillard JY. Use of hydrogen peroxide as a biocide: New consideration of its mechanisms of biocidal action. J Antimicrob Chemother 2012;67(7):1589–1596.
Lokhandwalla M, Sturtevant B. Mechanical haemolysis in shock wave lithotripsy (SWL): I. Analysis of cell deformation due to SWL flow-fields. Phys Med Biol 2001;46:413–437.
Lu J, Getz G, Miska EA, Alvarez-Saavedra E, Lamb J, Peck D, Sweet-Cordero A, Ebert BL, Mak RH, Ferrando AA, Downing JR, Jacks T, Horvitz HR, Golub TR. MicroRNA expression profiles classify human cancers. Nature 2005;435(7043):834–838.
Luo YK, Zhao YZ, Lu CT, Tang J, Li XK. Application of ultrasonic gas-filled liposomes in enhancing transfer for breast cancer-related antisense oligonucleotides: An experimental study. J Liposome Res 2008;18(4):341–351.
Lujambio A, Lowe SW. The microcosmos of cancer. Nature 2012;482(7385):347–355.
Ma Y, Zhang P, Yang J, Liu Z, Yang Z, Qin H. Candidate microRNA biomarkers in human colorectal cancer: Systematic review profiling studies and experimental validation. Int J Cancer 2012;130(9):2077–2087.
Mattie MD, Benz CC, Bowers J, Sensinger K, Wong L, Scott GK, Fedele V, Ginzinger D, Getts R, Haqq C. Optimized high-throughput microRNA expression profiling provides novel biomarker assessment of clinical prostate and breast cancer biopsies. Mol Cancer 2006;5:24.
Marmottant P, Hilgenfeldt S. Controlled vesicle deformation and lysis by single oscillating bubbles. Nature 2003;423:153–156.
National Cancer Institute, National Institute of Health. Tumor markers factsheet. Available at: http://www.cancer.gov/cancertopics/factsheet/detection/tumor-markers. Accessed March 6, 2012.
Nomikou N, McHale AP. Exploiting ultrasound-mediated effects in delivering targeted, site-specific cancer therapy. Cancer Lett 2010;296(2):133–143.
Ohl C-D, Arora M, Ikink R, de Jong R, Versluis M, Delius M, Lohse D. Sonoporation from jetting cavitation bubbles. Biophys J 2006;91:4285–4295.
Prentice P, Cuschieri A, Dholakia K, Prausnitz M, Campbell P. Membrane disruption by optically controlled microbubble cavitation. Nature Physics 2005;1:107–110.
Sassen S, Miska EA, Caldas C. MicroRNA—implications for cancer. Virchows Arch 2008;452(1):1–10.
Sheeran PS, Luois S, Dayton PA, Matsunaga TO. Formulation and acoustic studies of a new phase-shift agent for diagnostic and therapeutic ultrasound. Langmuir 2011;27:10412–10420.
Tainsky MA. Genomic and proteomic biomarkers for cancer: A multitude of opportunities. Biochim Biophys Acta 2009;1796(2):176–193.
Volinia S, Calin GA, Liu CG, Ambs S, Cimmino A, Petrocca F, Visone R, Iorio M, Roldo C, Ferracin M, Prueitt RL, Yanaihara N, Lanza G, Scarpa A, Vecchione A, Negrini M, Harris CC, Croce CM. A microRNA expression signature of human solid tumors defines cancer gene targets. Proc Natl Acad Sci USA 2006;103(7):2257–2261.
Wilson K, Homan K, Emelianov S. Biomedical photoacoustics beyond thermal expansion using triggered nanodroplet vaporization for contrast-enhanced imaging. Nature Commun 2012;3:618.
Wittmann J, Jäck HM. Serum microRNAs as powerful cancer biomarkers. Biochim Biophys Acta 2010;1806(2):200–207.
Wu J. Theoretical study on shear stress generated by microstreaming surrounding contrast agents attached to living cells. Ultrasound Med Biol 2002;28:125–129.
Yang F, Gu N, Chen D, Xi X, Zhang D, Li Y, Wu J. Experimental study on cell self-sealing during sonoporation. J Control Release 2008;131(3):205–210.
Yin T, Wang P, Zheng R, Zheng B, Cheng D, Zhang X, Shuai X. Nanobubbles for enhanced ultrasound imaging of tumors. Int J Nanomedicine 2012;7:895–904.
Zandberga E, Kozirovskis V, Abols A, Andrējeva D, Purkalne G, Linē A. Cell-free MicroRNAs as diagnostic, prognostic, and predictive biomarkers for lung cancer. Genes Chromosomes Cancer 2013;52(4):356–369.
Zhao YZ, Luo YK, Lu CT, Xu JF, Tang J, Zhang M, Zhang Y, Liang HD. Phospholipids-based microbubbles sonoporation pore size and reseal of cell membrane cultured in vitro. J Drug Target 2008;16(1):18–25.
Zhou Y, Kumon RE, Cui J, Deng CX. The size of sonoporation pores on the cell membrane. Ultrasound Med Biol 2009;35(10):1756–1760.